Since January 2020 Elsevier has created a COVID-19 resource centre with free information in English and Mandarin on the novel coronavirus COVID-19. The COVID-19 resource centre is hosted on Elsevier Connect, the company's public news and information website.

European Journal of Radiology 152 (2022) 110341

Contents lists available at ScienceDirect

European Journal of Radiology

journal homepage: www.elsevier.com/locate/ejrad

MR imaging spectrum in COVID associated Rhino-Orbito-Cerebral mucormycosis with special emphasis on intracranial disease and impact on patient prognosis

Apoorva Sehgal [a], Jyoti Kumar [a,*], Anju Garg [a], Ayush Jain [a], Ravi Meher [b], Meeta Singh [c], Ruchi Goel [d]

[a] Department of Radiodiagnosis, Maulana Azad Medical College and Lok Nayak Hospital, New Delhi 110002, India
[b] Department of ENT, Maulana Azad Medical College and Lok Nayak Hospital, New Delhi 110002, India
[c] Department of Pathology, Maulana Azad Medical College and Lok Nayak Hospital, New Delhi 110002, India
[d] Department of Ophthalmology, Maulana Azad Medical College and Guru Nanak Eye Centre, New Delhi 110002, India

ARTICLE INFO

Keywords:
COVID associated mucormycosis
Rhinoorbitocerebral mucormycosis
Invasive fungal sinusitis
Intracranial complication
Magnetic Resonance Imaging
Perineural spread
Fungal abscess

ABSTRACT

In the wake of the ongoing Coronavirus Disease 2019 (COVID-19) pandemic, a new epidemic of COVID associated mucormycosis (CAM) emerged in India. Early diagnosis and prompt treatment of this deadly disease are of paramount importance in improving patient survival. MRI is the cornerstone of diagnosis of early extrasinus disease, particularly intracranial complications which have traditionally been associated with a high mortality rate. In this review, we depict the sinonasal, perisinus, orbital and intracranial involvement in CAM. Special emphasis is laid on intracranial disease which is categorized into vascular, parenchymal, meningeal, bony involvement and perineural spread. Vascular complications are the most common form of intracranial involvement. Some unusual yet interesting imaging findings such as nerve abscesses involving the optic, trigeminal and mandibular nerves and long segment vasculitis of the internal carotid artery extending till its cervical segment are also illustrated. In our experience, patient outcome in CAM (survival rate of 88.5%) was better compared to the pre-pandemic era. Presence of intracranial disease also did not affect prognosis as poorly as traditionally expected (survival rate of 82.8%). Involvement of brain parenchyma was the only subset of intracranial involvement that was associated with higher mortality (p value 0.016). The aim of this review is to familiarise the reader with the MR imaging spectrum of CAM with special focus on intracranial complications and a brief account of their impact on patient prognosis in our experience.

1. Introduction

1.1. Background

Mucormycosis is an opportunistic potentially lethal infection caused by ubiquitous fungi of the order Mucorales which are commensals of the normal nasal mucosa but cause fulminant infection in an immunocompromised host [1]. Rhino-orbito-cerebral form of mucormycosis (ROCM) is the most common presentation, others being pulmonary, cutaneous, gastrointestinal and disseminated forms [2].

1.2. COVID associated mucormycosis (CAM) in the Indian context

India witnessed an unprecedented surge in cases of ROCM during the second wave of COVID–19 pandemic that hit India between March and July 2021 which led to this previously rare disease being declared as an epidemic in the country. The term COVID associated mucormycosis (CAM) was coined in view of this association. Review of existing literature reveals that 81% cases of CAM were reported from India [3]. Multiple plausable explanations include preexisting uncontrolled diabetes, COVID-19 induced diabetogenic state and immune dysregulation

Abbreviations: COVID, Coronavirus disease; CAM, COVID associated mucormycosis; MRI, Magnetic Resonance Imaging; ROCM, Rhino-orbito-cerebral mucormycosis; CT, Computed Tomography; RT-PCR, Reverse Transcriptase Polymerase Chain Reaction; ICA, Internal carotid artery; FLAIR, Fluid attenuation inversion recovery; SWI, Susceptibility weighted imaging; ADC, Apparent Diffusion Coefficient; STIR, Short Tau Inversion Recovery.

* Corresponding author.
E-mail address: drjyotikumar@gmail.com (J. Kumar).

https://doi.org/10.1016/j.ejrad.2022.110341
Received 28 December 2021; Received in revised form 10 April 2022; Accepted 1 May 2022
Available online 6 May 2022

Table 1
MRI Protocol

Sequence	TR (ms)	TE (ms)	Flip Angle (°)	Acquisition matrix	FOV (mm)	Slice thickness (mm)	Intersection gap (mm)	NEX
PNS and Orbit———								
T1 TSE axial	450–600	7.1–9.2	150	256x256	160	3	0.5	2
T1 TSE fat-sat coronal	450–600	7.1–9.2	150	256x256	160	3	0.5	2
T2 TSE fat-sat axial	4000–4200	79	150	384x384	180	3	0.6	3
Axial DWI (Multishot echoplanar RESOLVE sequence at b values- 0,1000 s/mm^2)	5500	64	180	160x160	220	4	1.2	1
Post contrast T1 TSE fat-sat axial, coronal	450–600	7.1–9.2	150	256x256	160	3	0.3	3
Brain———								
T2 TSE axial	6000	99	150	320x320	220	4	1.2	1
FLAIR coronal	9000	81	150	320x320	220	4	1.6	1
T1 TSE sagittal	2000	9	150	320x320	240	4	1.2	1
Axial SWI	27	20	15	256x256	220	2	0.4	1
Axial DWI (Single Shot echoplanar sequence at b values- 0,1000 s/mm^2)	7000	98	–	192x192	220	4	1.2	3
3D multislab TOF angiography	21	3.4	18	384x384	200	0.5	−0.5	1
Post contrast MPRAGE	1660	2.47	8	256x256	230	1	0.5	1

*TSE- Turbo spin echo.
DWI- Diffusion weighted imaging.
RESOLVE- Readout segmentation of long variable echo-trains.
FLAIR-Fluid attenuation inversion recovery.
SWI- Susceptibility weighted imaging.
TOF- Time of flight.
MPRAGE- Magnetization-prepared rapid gradient-echo.

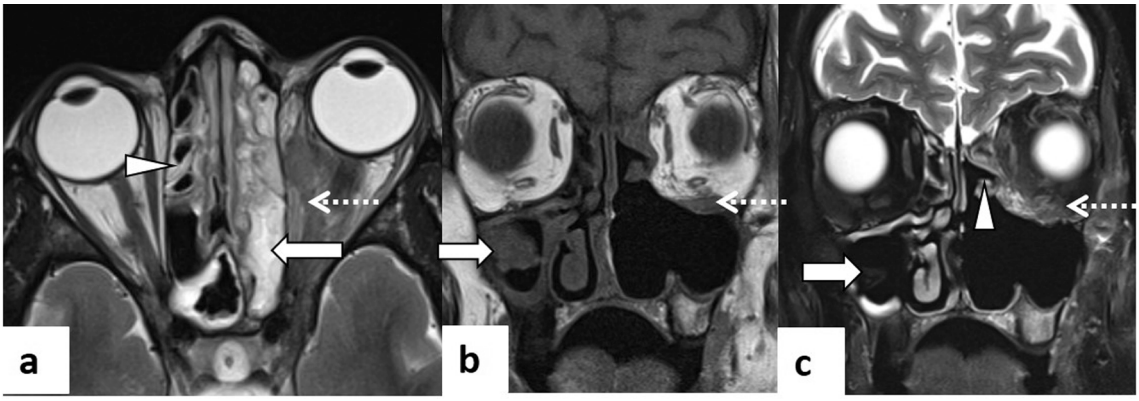

Fig. 1. Rhino-orbital involvement in two patients with CAM. Axial T2W MR image (a) reveals heterogeneously hyperintense mucosal thickening in left ethmoid sinus (arrow) with extrasinus extension into left orbit (dashed arrow). Non-specific mucosal thickening is noted in right ethmoid sinus (arrowhead). In another patient with CAM, post debridement, coronal T1 (b) and T2FS MR images (c) show mucosal thickening in right maxillary sinus with paramagnetic fungal elements within appearing isointense on T1 and markedly hypointense on T2W image (arrow). Left ethmoid sinusitis is also seen (arrowhead) with extension into inferomedial extraconal left orbit (dashed arrow).

in the form of raised immature neutrophil count, incompetent innate immune system, decreased CD4 and CD8 cell counts, high ferritin levels and the injudicious use of steroids for the treatment of COVID pneumonia. The rampant use of zinc and iron containing supplements, industrial oxygen and contaminated oxygen humidifiers have also been speculated as other probable causes [4].

1.3. Etiopathogenesis, epidemiology and clinical features of CAM

The fungal spores are inhaled into the nasopharynx following which tissue invasion, thrombosis and necrosis progress from the nose to paranasal sinuses, orbit and brain. As per the current literature, the disease mostly affects middle aged males with majority of them presenting within 10–14 days of testing positive for COVID-19 [3,5].

Clinical symptoms of sinonasal and perisinus involvement include nasal stuffiness, foul smell, epistaxis, black nasal discharge, nasal mucosal discolouration or eschar, loosening of tooth, facial pain or swelling and paresthesia. Patients with orbital disease usually present with proptosis, ptosis, sudden loss of vision and diplopia. Once the infection has spread to the brain, patients may present with headache, altered sensorium, paralysis, cranial nerve palsy and focal seizures [6,7]. Intracranial disease is associated with dismal prognosis with the patient mortality reaching upto 80% in various studies in the pre-pandemic era [8]. This warrants early diagnosis and checking disease progression in its early stages by aggressive medical and/or surgical management.

1.4. Diagnosis

Although the definitive diagnosis of mucormycosis is made on histopathology and fungal culture, the role of imaging in prompt diagnosis,

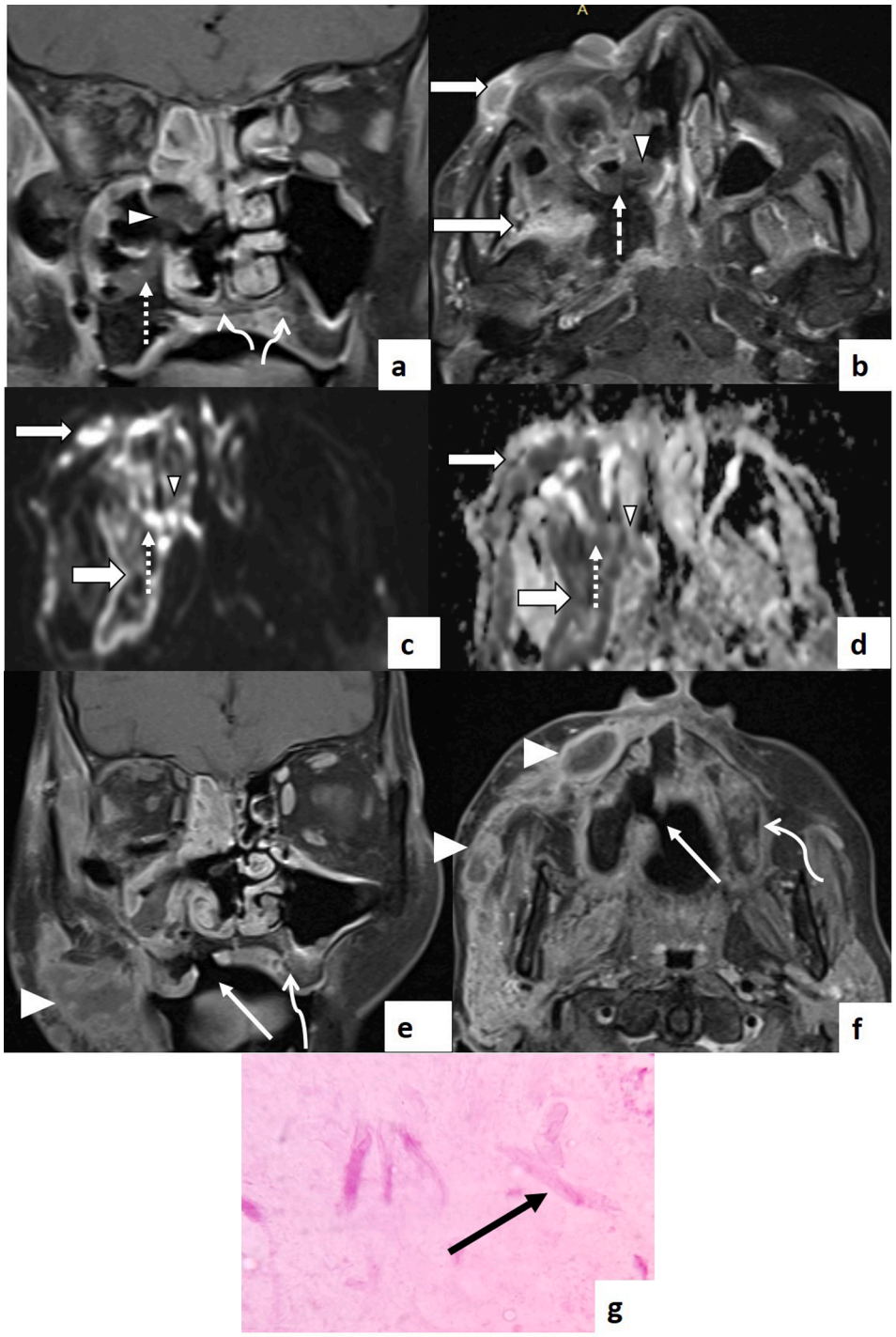

Fig. 2. 'Black turbinate sign' and oroantral fistula in CAM. Post contrast coronal (a) and axial T1FS MR images (b) reveal lack of contrast enhancement in right middle turbinate (arrowhead) and maxillary sinus mucosa (dashed arrow)-'black turbinate sign'. Axial DWI (c) shows hyperintensity with signal drop on corresponding ADC map (d) suggestive of diffusion restriction in the regions of the non-enhancing sinonasal mucosa. Extrasinus extension is noted in the form of hard palate (curved arrows in a) and periantral fat involvement (arrow in b,c,d). Coronal (e) and axial post contrast MR images (f) in the same patient show extensive involvement of the hard palate (curved arrow) with oroantral fistula on right (straight arrow) and ulceration in the adjacent palatal mucosa. Soft tissue abscesses are noted along the right cheek (arrowhead). High power (x400) hematoxylin and eosin stained section of the sinonasal mucosa (g) shows irregular branching fungal hyphae (arrow) in a background of necrosis.

Table 2
Association of sinonasal and orbital disease with intracranial involvement.

SINONASAL INVOLVEMENT (n= 31 patients as post-debridement patients were excluded)				
Site of involvement	Patients with intracranial involvement n = 19 (%)	Patients without intracranial involvement n = 12 (%)	p value	Total n = 31 (%)
Ethmoid sinus	15 (78.9)	8 (66.7)	0.45	23 (74.2)
Maxillary sinus	12 (63.2)	9 (75)	0.49	21 (67.7)
Sphenoid sinus	12 (63.2)	5 (41.7)	0.24	17 (54.8)
Frontal sinus	7 (36.8)	5 (41.7)	0.79	12 (38.7)
Nasal cavity	15 (78.9)	7 (58.3)	0.22	22 (71)
ORBITAL INVOLVEMENT (n=52 patients)				
Site of involvement	**Patients with intracranial involvement n = 29 (%)**	**Patients without intracranial involvement n = 23 (%)**	**p value**	**Total n = 52 (%)**
Anterior orbit alone	18 (62.1)	9 (39.1)	0.1	27 (51.9)
Orbital apex ± anterior orbit	25 (86.2)	9 (39.1)	**0.0004**	34 (65.4)

defining disease extent, early identification of complications as well as follow up is imperative. MRI with its exquisite soft tissue contrast resolution is the imaging modality of choice to detect early extrasinus extension particularly intracranial disease in the setting of CAM [9]. Except for cortical bone involvement, MRI has higher sensitivity for detecting all intracranial complications of CAM as compared to CT.

1.5. Management

The management of CAM involves prompt medical management along with surgical debridement and control of risk factors such as hyperglycemia. Liposomal Amphotericin B, Posaconazole and Voriconazole are some of the anti-fungal agents used for treatment. Surgical intervention may be performed by endoscopic, open or combined approaches. Mapping of the disease extent on imaging remains crucial for deciding the surgical approach. The various surgeries include Functional Endoscopic Sinus Surgery (FESS), maxillectomy, orbital debridement and exenteration. This is followed by regular suction in the postoperative period to clear the residual disease with oral posaconazole and weekly nasal endoscopy after discharge [4].

The indications for neurosurgical intervention include relief of raised intracranial pressure, drainage of obstructive hydrocephalus and excision of lesions compressing the spinal cord. Radical excision of fungal brain abscess is best avoided. Decompressive hemicraniectomy may be performed where elevated intracranial pressure and impending herniation are concerns [10].

2. Materials and methods

A total of 52 patients with CAM were included in this review of which 29 patients had intracranial disease on MR examination.

All 52 patients were histopathologically proven cases of ROCM with a history of RT-PCR positive COVID-19 infection in the past 4–6 weeks. None of the patients had active COVID-19 infection at the time of examination.

2.1. MRI technique

MRI of the paranasal sinuses, orbit and brain was performed on 3 T Scanner -MAGNETOM Skyra (Siemens Healthcare, Erlangen, Germany) using a dedicated 32 channel phased array head coil after administration of 0.1–0.2 mmol/kg body weight of Gadopentetate dimeglumine (Magnascan, Unijules Life Sciences Ltd, India). The detailed protocol is given in Table 1.

3. MR imaging findings

Based on anatomic involvement, disease spread in CAM can be

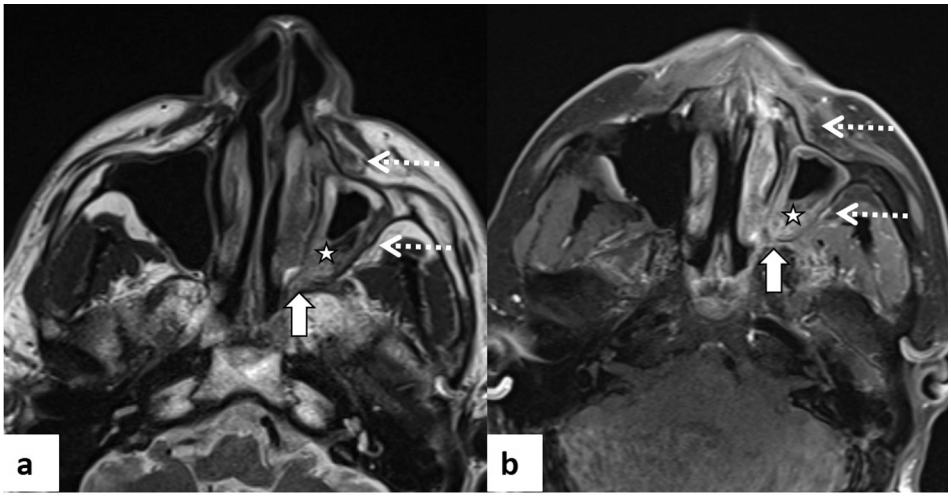

Fig. 3. Early anterior and posterior periantral involvement in CAM. Axial T2W (a) and post contrast T1FS MR images (b) show left maxillary sinusitis (*) with anterior and posterior periantral fat involvement (dashed arrow). Heterogeneity and enhancement are also seen in the left pterygopalatine fossa (arrow).

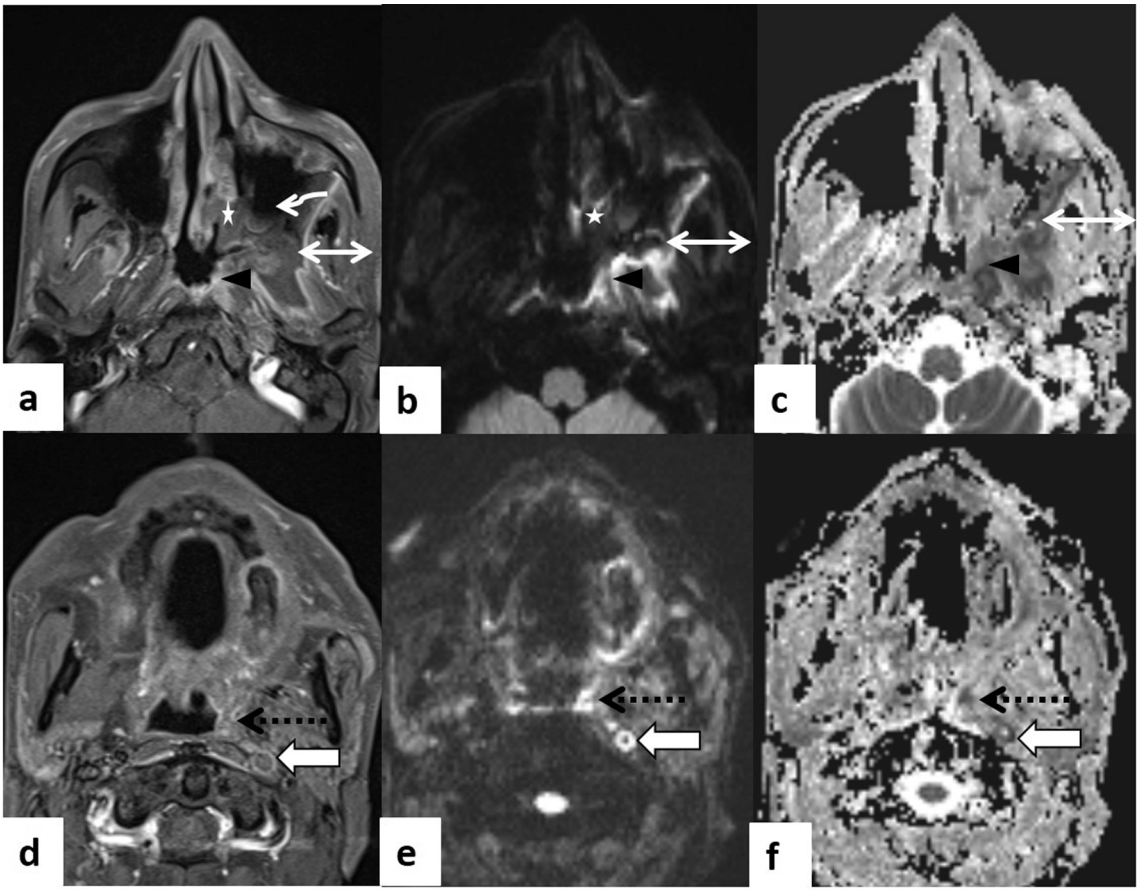

Fig. 4. Carotid space involvement in CAM. Axial post contrast T1FS MR image (a), DWI (b) and corresponding ADC map (c) show mucosal disease in left maxillary sinus (curved arrow) and nasal cavity (*)with a peripherally enhancing abscess in left posterior periantral space (double arrow) and nasopharyngeal mucosal involvement (arrowhead). Inferiorly, axial post contrast image (d), DWI (e) and ADC map (f) reveal the involvement of the left oropharyngeal mucosal (dashed arrow) and carotid space (arrow). Note the characteristic restriction of diffusion in the walls of the left internal carotid artery (arrow in e, f) suggestive of inflammation of the vessel wall-vasculitis.

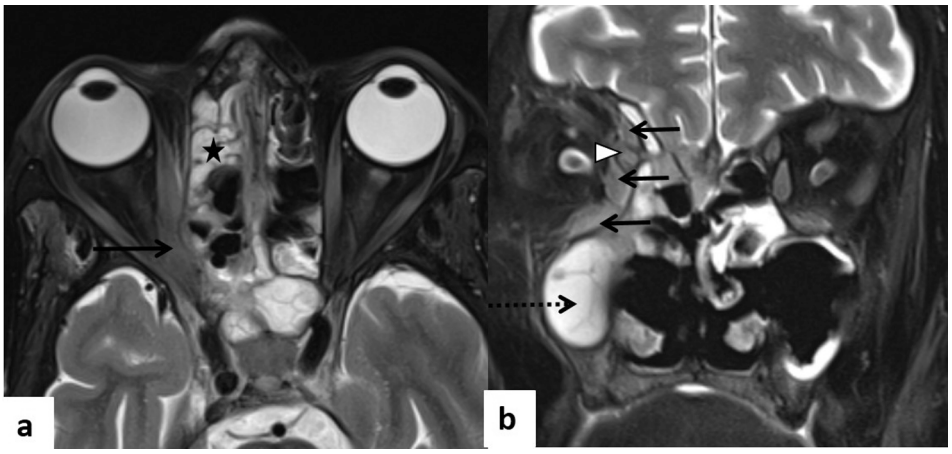

Fig. 5. Early orbital involvement in CAM. Axial (a) and coronal (b) T2FS MR images in a patient with CAM, post debridement, show right ethmoid (*) and maxillary sinusitis (dashed arrow) with inflammatory soft tissue and heterogeneity in inferomedial aspect of extraconal space of right orbit (arrowhead). Note the involvement of the extraocular muscles- superior oblique, medial and inferior recti (arrow) which appear bulky with surrounding fat stranding. Mucosal thickening is also noted in left ethmoid and maxillary sinuses.

classified as sinonasal, perisinus, orbital and intracranial.

3.1. Sinonasal disease

Sinonasal disease presents as mucoperiosteal thickening showing variable signal intensity on T1 and T2 weighted MR images. T1 hyperintensity and T2 hypointensity can be attributed to paramagnetic fungal elements (Fig. 1). T2 hyperintensity with restriction of diffusion and lack of contrast enhancement, known as the *'black turbinate sign'* are pointers towards necrotic divitalized tissue on histopathology [5,10] (Fig. 2). Bony changes may be seen in the form of cortical erosions or

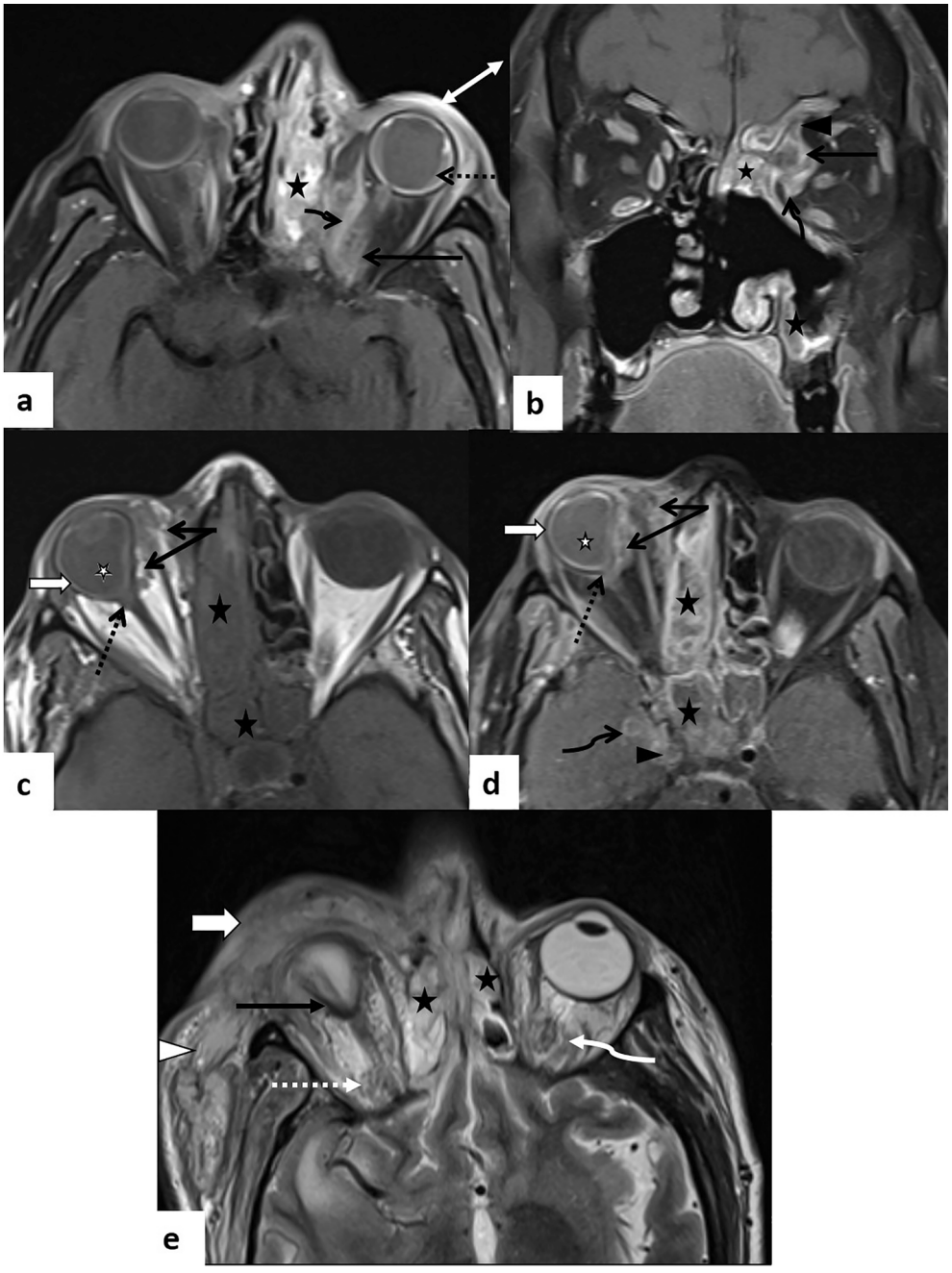

Fig. 6. Extensive orbital involvement in three patients with CAM. In a patient with CAM, post debridement, axial (a) and coronal (b) T1FS MR images depict left ethmoid and maxillary sinusitis (*) with a peripherally enhancing abscess in medial extraconal space of left orbit (arrow) and inflammatory changes in the medial rectus (curved arrow) and superior oblique (arrowhead) muscles. Associated left choroidal detachment (dashed arrow) with suprachoroidal collection and inflammatory changes in the preseptal space (double arrow) are seen. Axial pre- (c) and post contrast T1W MR images (d) in another patient show heterogeneously enhancing inflammatory soft tissue in medial extraconal and intraconal spaces of right orbit (arrow) with resultant deformation of the right ocular globe (dashed arrow). Associated uveoscleral thickening (white block arrow) and T1 hyperintensity of the vitreous (white *) is seen in right globe as compared to left suggestive of panophthalmitis. Note made of right ethmoid and sphenoid sinusitis (black *) with right ICA thrombosis (arrowhead) and enhancing soft tissue along the paracavernous dura (curved arrow). Axial T2W MR image (e) in a third patient shows extensive right pre-septal (white block arrow) and post-septal cellulitis (white dashed arrow) with inflammation extending into the *peri*-orbital region (arrowhead) and posterior tenting of the ocular globe giving the 'guitar pick sign' (black arrow) suggestive of orbital compartment syndrome. Note made of bilateral ethmoid sinusitis (*) with left post-septal cellulitis (curved arrow).

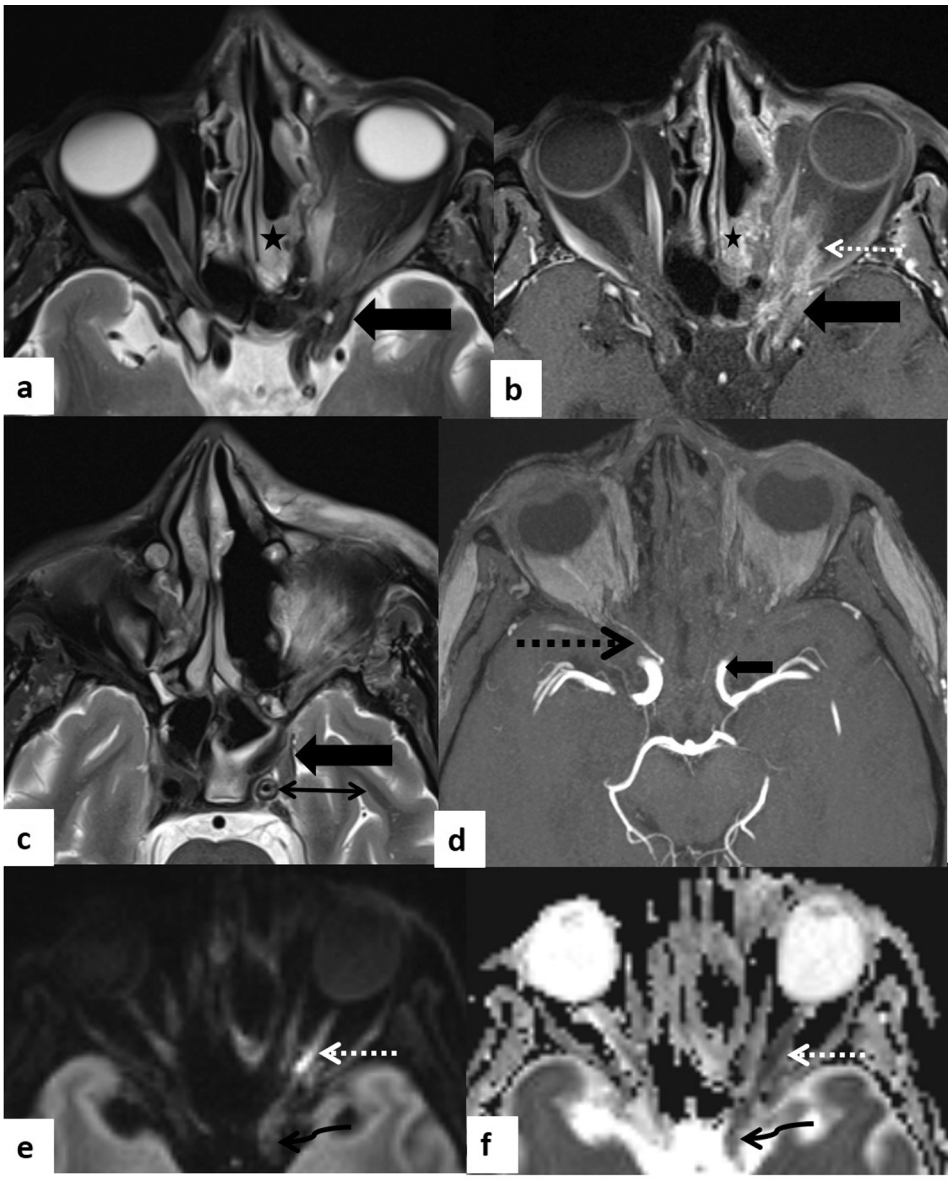

Fig. 7. Orbital apex disease with optic nerve ischemia in CAM. Axial T2FS (a) and post contrast T1FS MR images (b) in a patient with CAM, post debridement, reveal left posterior ethmoid sinusitis (*) with inflammatory changes in the intraconal space of left orbit (dashed arrow) encasing the optic nerve and extending posteriorly till the orbital apex (arrow). Axial T2FS image at a lower level (c) shows involvement of the left cavernous sinus (arrow) which appears bulky with wall thickening in the ipsilateral ICA (double arrow) suggestive of vasculitis. Axial TOF angiography image (d) depicts non-visualization of the left ophthalmic artery suggestive of thrombosis in the presence of a patent but mildly attenuated ipsilateral ICA (arrow). Note the normal right ophthalmic artery (dashed arrow). Axial DWI (e) and corresponding ADC map (f) show diffusion restriction in the left intraorbital (dashed arrow) and pre-chiasmatic intracranial optic nerve (curved arrow) indicating resultant optic nerve ischemia.

bone marrow signal alteration. Middle turbinate is the commonest site of involvement in the nasal cavity while maxillary, ethmoid and sphenoid sinuses are the commonly affected paranasal sinuses [11]. In our study group, ethmoid sinuses were the most commonly involved followed by maxillary, sphenoid and frontal sinuses. No significant difference in the distribution of sinonasal involvement was seen between patients with and without intracranial disease (Table 2). Few studies have however proposed a greater risk of intracranial spread from ethmoid and sphenoid sinuses via the orbit/cribriform plate and cavernous sinus respectively [12].

3.2. *Perisinus disease*

Extrasinus extension is the hallmark of CAM and this can occur without frank bony destruction due to its angioinvasive propensity and ability to disseminate along perivascular and perineural channels. Preantral and retroantral fat, sphenopalatine foramen, nasopharynx, pterygopalatine and infratemporal fossa, buccal space, masticator space, palate and oral cavity should be evaluated for disease spread. Early involvement may be seen as obliteration of fat planes, stranding and inflammatory edema (Fig. 3) which may progress to abscess formation, osteomyelitis with cortical erosions and oroantral/oronasal fistula in advanced disease [5,13] (Figs. 2, 4).

3.3. *Orbital disease*

Disease spread to the orbit can occur via various neurovascular foramina/ fissures in the orbital walls that include anterior and posterior ethmoidal foramen along the medial orbital wall, infraorbital foramen along the floor, inferior orbital fissure along the inferolateral wall as well as nasolacrimal duct along the inferomedial wall of the orbit [14]. Orbital spread secondary to bone destruction was rarely encountered in CAM. Understandably, the earliest signs of orbital involvement depend on the route of disease spread. Spectrum of orbital disease in CAM

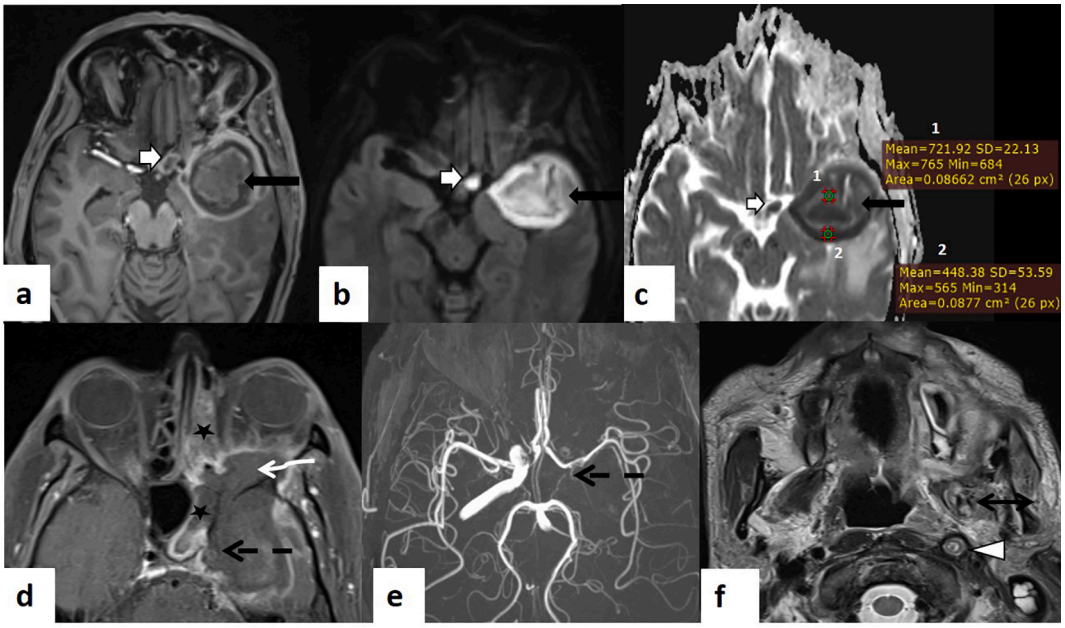

Fig. 8. Parenchymal and optic nerve abscess with ICA thrombosis in CAM. Axial post-contrast T1FS image (a), DWI (b) and corresponding ADC map (c) show a rim-enhancing abscess with restricted diffusion involving the left temporal lobe (black arrow in a, b, c) and prechiasmatic left optic nerve (white arrow in a, b, c). The centre of the abscess cavity shows higher mean ADC value of 0.72 × 10^{-3}mm^2/s (ROI 1) as compared to its wall which has a mean ADC value of 0.45 × 10^{-3}mm^2/s (ROI 2). Parenchymal abscess is seen to extend into the left orbit (curved arrow in d) and cavernous sinus with ICA thrombosis (dashed arrow in d, e) on axial post-contrast (d) and TOF angiography images (e). Note the long segment thrombosis of left ICA extending to its cervical segment with associated vessel wall thickening on axial T2W image (arrowhead in f). Left ethmoid and sphenoid sinusitis (* in d) with involvement of masticator space (double arrow in f) is noted.

Table 3
INTRACRANIAL COMPLICATIONS AND THEIR IMPACT ON PATIENT OUTCOME (n = 29 patients, but more than one complication encountered in majority of the patients).

Intracranial complication	Frequency (%)	Survived	Deceased	p value
VASCULAR	**22 (75.9)**	18	4	0.9
• **Venous thrombosis**				
-Cavernous sinus	18 (62.1)			
-Cortical vein	1 (3.4)			
• **Arterial thrombosis**				
-ICA	8 (27.6)			
-ACA	1 (3.4)			
-MCA	2 (6.9)			
• **Basilar artery encasement**	1 (3.4)			
• **ICA vasculitis**	5 (17.2)			
Parenchymal	**14 (48.3)**	9	5	**0.016**
• Infarct	8 (27.5)			
• Abscess	7 (24.1)			
• Mucor emboli	2 (6.9)			
Meningeal	**11 (37.9)**	8	3	0.3
• Focal pachymeningitis	8 (27.6)			
• Focal leptomeningitis	3 (10.3)			
• Dural abscess	2 (6.9)			
Bony	**18 (62.1)**	13	5	0.1
• Marrow signal abnormality	15 (51.7)			
• Cortical destruction	3 (10.3)			
• Subperiosteal abscess	1 (3.4)			
Perineural spread	**13 (44.8)**	10	3	0.6
• Nerve abscess	4 (13.8)			

*ACA- anterior cerebral artery.
*MCA- middle cerebral artery.

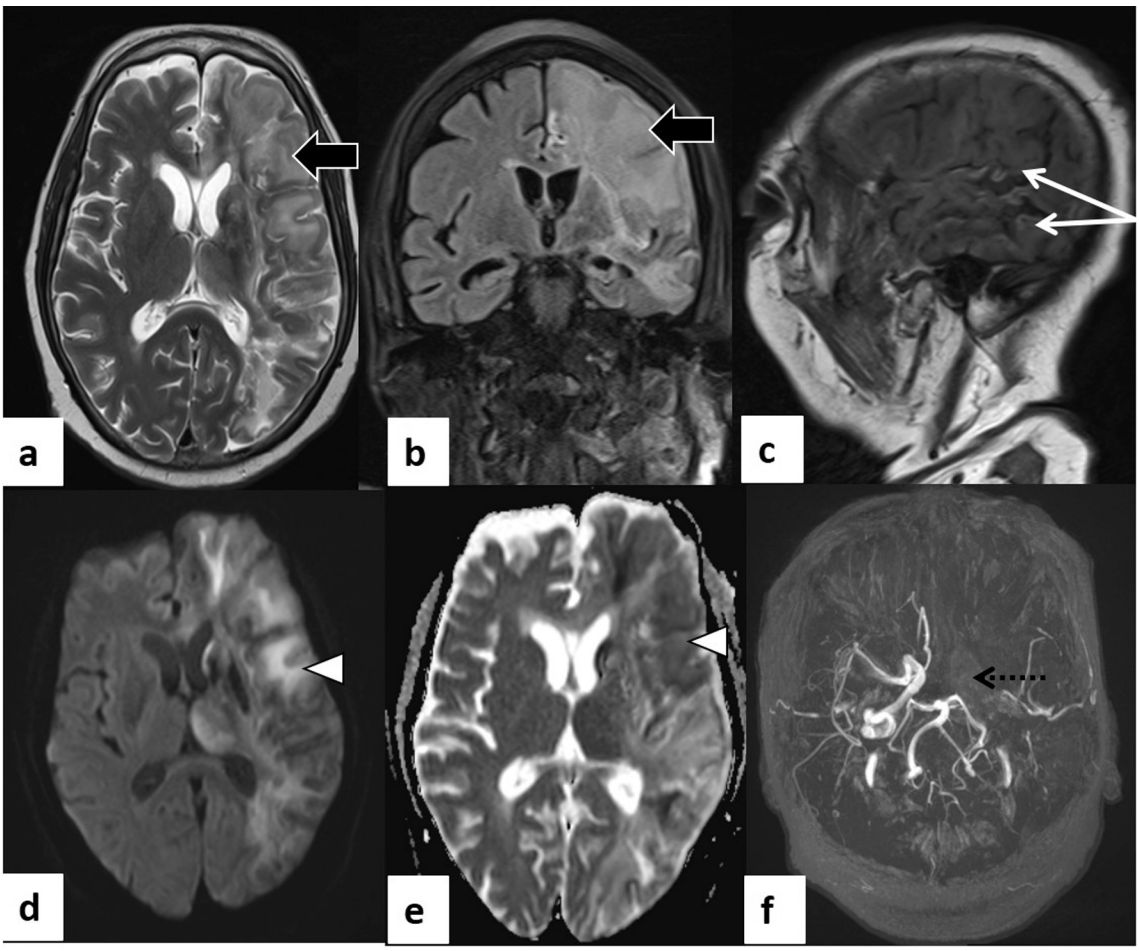

Fig. 9. Anterior circulation infarct in CAM. Axial T2 (a) and coronal FLAIR MR images (b) reveal hyperintensity involving the left cerebral hemisphere and gangliothalamic complex with loss of grey-white matter differentiation (block arrow), gyriform cortical T1 hyperintensity (white arrow) on sagittal T1W image (c) and diffusion restriction (arrowhead) on DWI (d) and corresponding ADC map (e). There is complete non-visualization of left ICA, ACA and MCA (dashed arrow) on TOF angiography image (f) suggestive of complete left ICA thrombosis with infarction and cortical laminar necrosis.

includes involvement of the extraocular muscles (superior oblique is usually the first to be involved due to its proximity to the anterior ethmoidal foramen in the lamina papyracea), extraconal and intraconal fat (inflammation in medial and inferior extraconal fat along with involvement of lacrimal sac are early signs of orbital disease), optic nerve, globe, orbital apex and bony orbital walls [5,13]. Orbital fat involvement can be seen as stranding, soft tissue infiltration or abscess formation (Figs. 5, 6).The occlusion of the ophthalmic artery and/or central retinal artery may result in optic nerve infarction which is seen as altered T1 and T2 signal intensity of the involved nerve with diffusion restriction [15] (Fig. 7). Optic neuritis appears as thickening and enhancement of the optic nerve sheath.

We encountered nerve abscess involving the pre-chiasmatic optic nerve in two patients. This was an interesting, yet uncommon complication of CAM. The involved nerves appeared bulky with peripheral enhancement, central liquefaction and diffusion restriction (Fig. 8). Detailed literature search yielded only few case reports of nerve abscesses involving the trigeminal and optic nerves in the pre-pandemic era with a single documented case report in CAM [16,17].

Uveoscleral thickening with tenting of the posterior pole of the globe (*'guitar pick sign'*) is an imaging feature of orbital compartment syndrome, a dreaded complication of orbital disease in CAM [13] (Fig. 6).

3.4. Intracranial disease

Intracranial spread of the fungus can occur either via the orbital apex, cribriform plate of ethmoid or across the bony walls of frontal and sphenoid sinuses. Angioinvasion and perineural spread are other important means of intracranial spread [18]. In our study group, orbital apex was the most important conduit for intracranial disease spread. It was involved in 86.2% (25/29) patients with intracranial disease and 39.1 % (9/23) patients without intracranial involvement (p value 0.0004). Thus, careful evaluation of the apex is of paramount importance. [5] (Table 2, Fig. 7).

The spectrum of intracranial disease can be categorized as vascular, parenchymal, meningeal, bony involvement and perinerual spread. Table 3 summarizes the frequency of various intracranial complications in our study group and their impact on patient outcome.

A) Vascular involvement

a) **Venous thrombosis-** Cavernous sinus thrombosis is a frequent vascular complication of CAM. Signs of cavernous sinus involvement include increase in bulk with lateral convexity of its wall, abnormal signal intensity on T1 and T2 weighted images and filling defects on post contrast study. Ancillary findings of a dilated and thrombosed superior ophthalmic vein and luminal attenuation of the ipsilateral internal carotid artery (ICA) with or without thrombosis and vasculitis may be seen. Paracavernous soft tissue may also be seen [19,20,21] (Fig. 6c, 6d, 7 and 8). Other dural venous sinus thrombosis can similarly be seen as loss of flow void on T2/T2 FLAIR spin echo sequences, filling defect on post contrast images (*'empty delta*

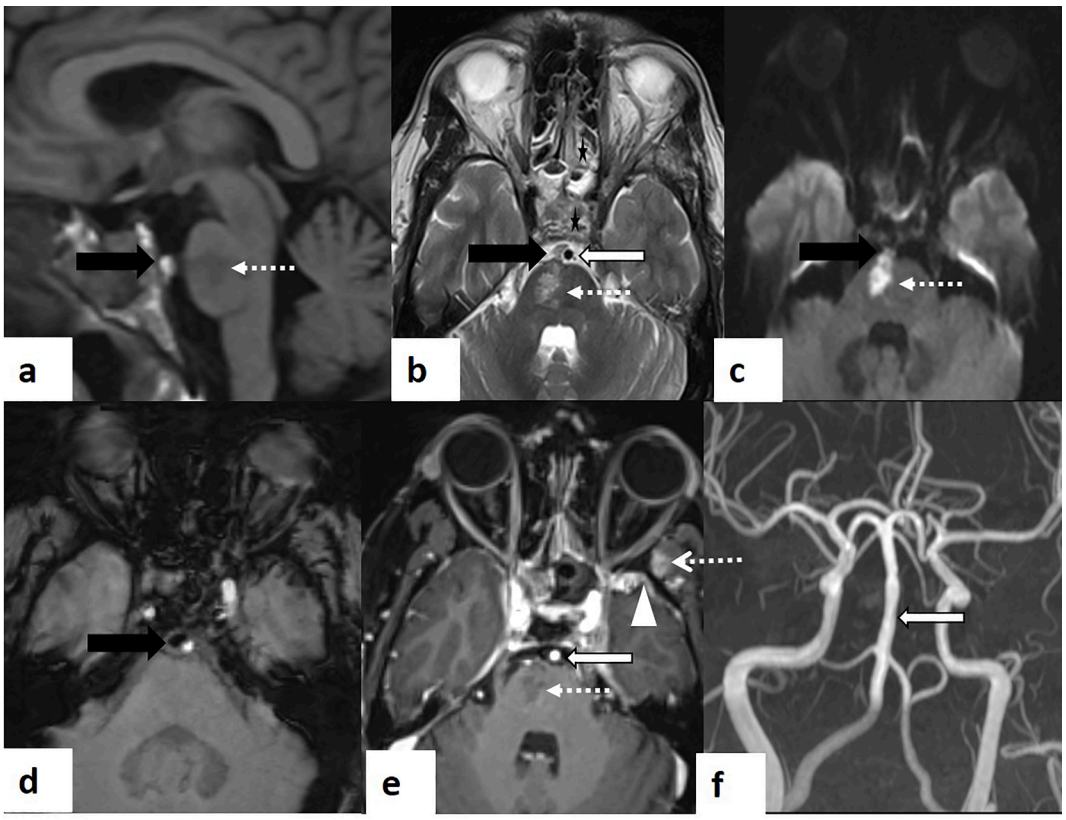

Fig. 10. Posterior circulation infarct in CAM. MR images demonstrate acute pontine infarct (dashed arrow) appearing hypointense on sagittal T1 W (a), hyperintense on axial T2W image (b) with diffusion restriction on DWI (c) and no post contrast enhancement (e). Soft tissue surrounding the basilar artery is seen in the prepontine cistern (black arrow in a,b,c,d), appearing hyperintense on T1, hypointense on T2 with diffusion restriction on DWI and blooming on SWI (d). However, basilar artery (white arrow in b, e, f) shows normal flow void, calibre and enhancement on T2 W (b), TOF angiography (f) and post-contrast image (e) respectively. Note made of T2 hypointense contents in sphenoid sinus and bilateral posterior ethmoid air cells (* in b) with focal pachymeningitis along left temporal lobe (arrowhead in e) and involvement of left temporal fossa (dashed arrow in e).

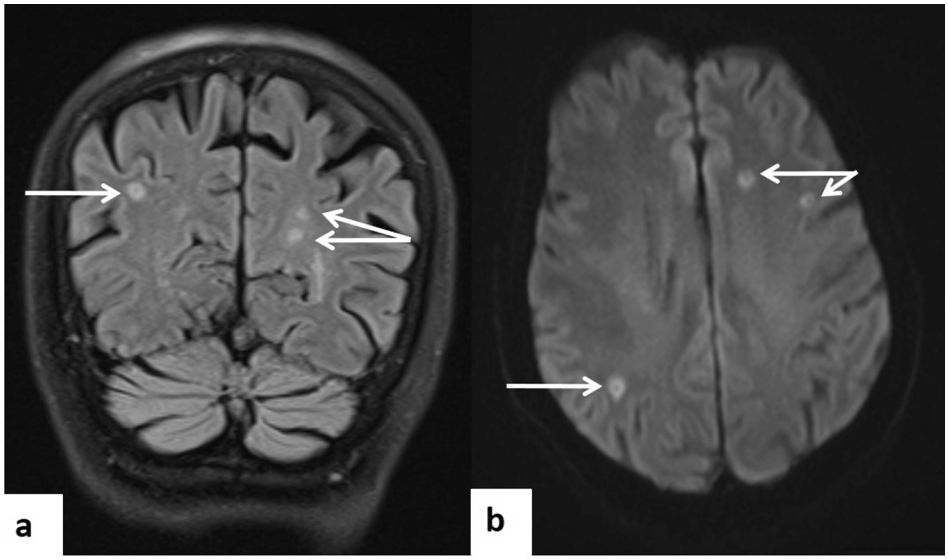

Fig. 11. Mucor emboli in CAM. Coronal FLAIR image (a) shows multiple, tiny, round hyperintense mucor emboli (arrow) at grey-white matter junction of bilateral cerebral hemispheres with diffusion restriction on DWI (b).

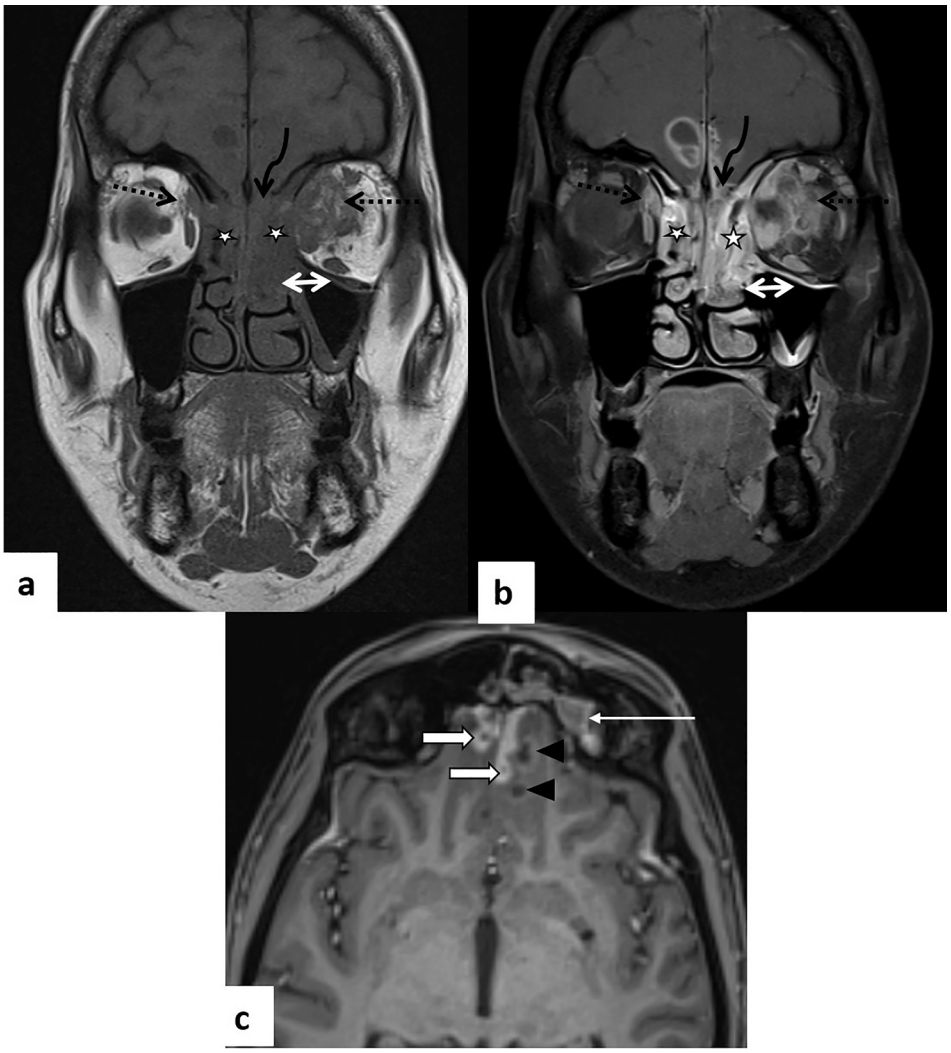

Fig. 12. Dural abscess in CAM. Coronal T1W (a) and post contrast coronal (b) and axial (c) T1FS MR images reveal sinonasal disease in bilateral ethmoid (*), left frontal sinus (thin white arrow) and nasal cavity (double arrow) with extension into bilateral orbits (dashed arrow). There is non-visualization of the cribriform plate of ethmoid (curved arrow) with contiguous intracranial disease spread in the form of few peripherally enhancing dural based (white block arrow) and parenchymal (arrowhead) granulomas/ abscesses in bilateral basifrontal regions.

sign') and blooming on susceptibility weighted images (SWI). SWI is particularly important for depicting cortical venous thrombosis, another vascular complication of CAM [5].

b) **Arteritis, arterial thrombosis and aneurysm**- Involvement of the cavernous segment of internal carotid artery occurs commonly with cavernous sinus as well as orbital apex involvement [20] (Fig. 7). Imaging features on MR include enhancement and thickening of its wall (vasculitis) causing luminal compromise, progressing to complete thrombosis which appears as loss of normal flow void and absence of contrast enhancement on spin echo and post contrast images respectively [19] (Fig. 6c,d, 7 and 8). Interestingly, we encountered long segment ICA vasculitis, involving its entire cervical segment in one case (Fig. 8). To the best of our knowledge, such long segment vasculitis has not been previously reported. Other intracerebral vessels may also be similarly involved, though involvement of the posterior circulation is less common [22]. In our study, posterior circulation was involved in one patient with pontine infarct where soft tissue was seen encasing the basilar artery in the prepontine cistern. However, no luminal attenuation or filling defect in the basilar artery was appreciated on MRI (Fig. 10). This may be attributed to the presence of microscopic thrombus in the basilar artery or involvement of its branches which could not be depicted on MRI. Arterial aneurysm and resultant subarachnoid or intracerebral hemorrhage due to aneurysmal rupture are other life threatening vascular complications [5,13].

B) Parenchymal involvement

a) **Infarct-**Vascular involvement results in ischemic infarcts which may be the result of direct vascular invasion or embolism in case of hematogenous dissemination of the fungus [19]. In our experience, arterial infarcts were more common than venous infarcts with predominant involvement of the anterior circulation. The commonest territory involved was that of middle cerebral artery (50%) followed by watershed territories (25%). Isolated cases of posterior cerebral artery and basilar artery territory infarcts were also seen. Although uncommon, these have been previously described with ROCM [20,22]. Acute arterial infarcts are seen as areas of T2/FLAIR hyperintensity and restricted diffusion with loss of grey-white matter differentiation in a specific vascular territory. Subsequently, the infarcted areas may show gyriform cortical T1 hyperintensity suggestive of cortical laminar necrosis and hemorrhagic transformation, best visualized on SWI (Figs. 9, 10).

b) **Cerebritis and abscess-** On MRI, early cerebritis appears as cortical-subcortical T1 iso-hypointense, T2/FLAIR hyperintense areas in a non-vascular distribution with patchy restricted diffusion and no contrast enhancement. Progressive peripheral enhancement may be seen in late cerebritis stage which may then progress to frank abscess formation. The latter is seen as peripherally enhancing centrally liquefied collection with non-enhancing intracavitary projections. Both the wall and the mural projections typically show restricted

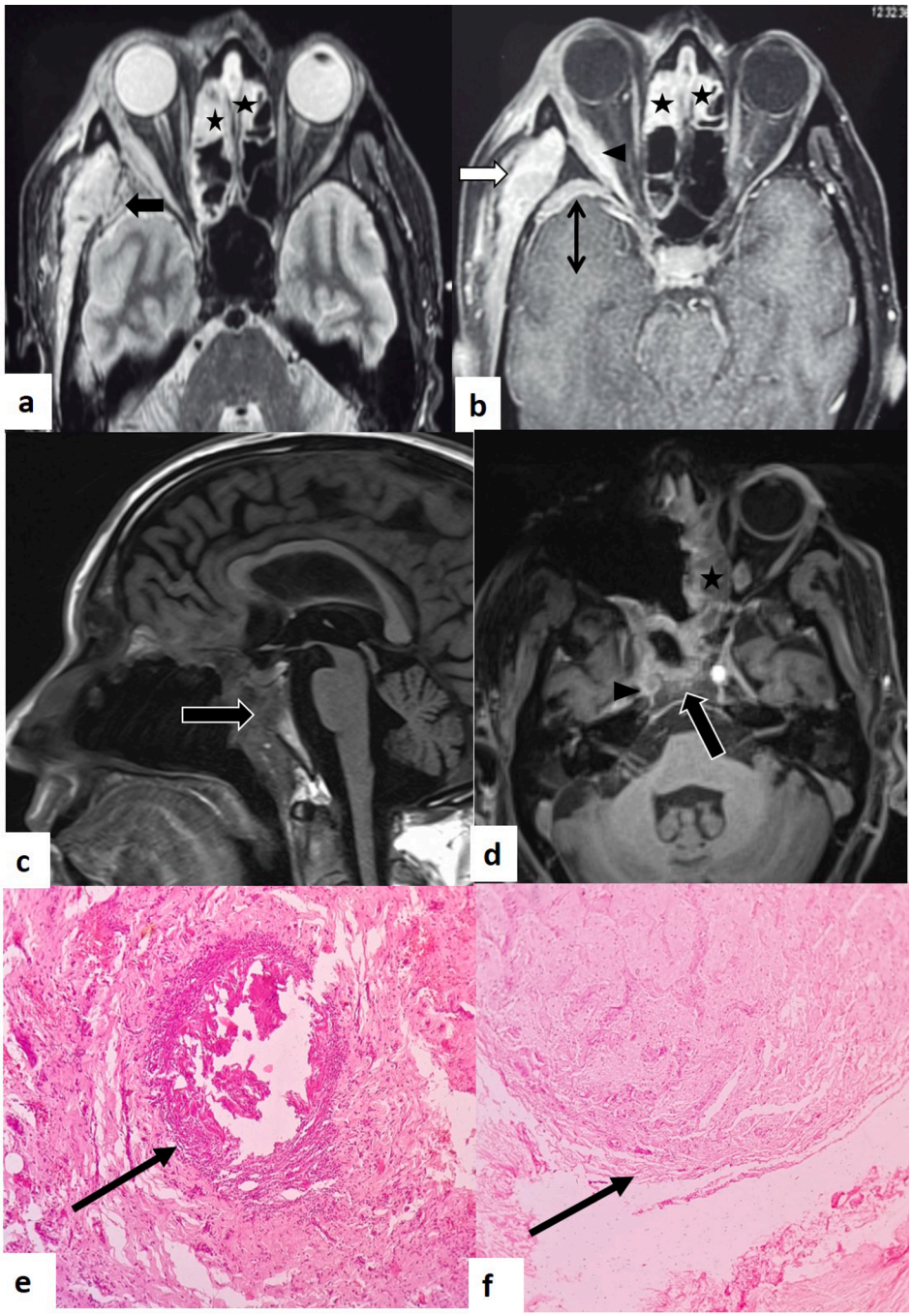

Fig. 13. Skull base osteomyelitis in two patients with CAM. Axial T2W (a) and post-contrast T1FS image (b) in a patient with CAM show marrow signal alteration in right greater wing of sphenoid (arrow in a) with associated enhancing phlegmonous collection extending into the extraconal orbit, intracranial extradural space and temporal fossa (arrowhead, double arrow and block arrow in b respectively). Note made of bilateral ethmoid sinusitis (*).Sagittal T1 (c) and post contrast axial T1FS MR images (d) in another patient with CAM post orbital exenteration, depict marrow signal alteration involving the clivus appearing hypointense on T1 with post contrast enhancement (arrow in c,d). Right ICA thrombosis (arrowhead in d) and left ethmoid sinusitis (* in d) is noted. High power (x400) hematoxylin and eosin stained section of the sinonasal mucosa (e) in second patient shows angioinvasion by fungal hyphae (arrow). High power (x400) hematoxylin and eosin stained section of nerve (f) in the second patient shows perineural invasion by fungal hyphae (arrow).

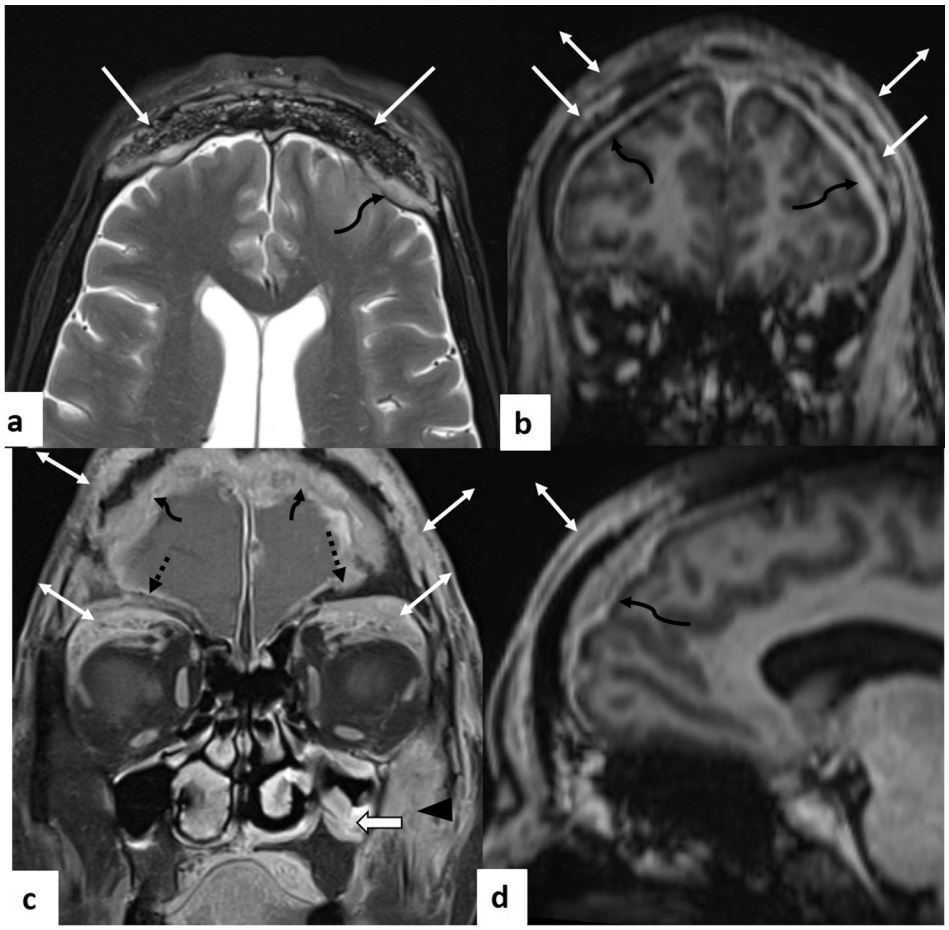

Fig. 14. Frontal bone osteomyelitis in CAM. Axial STIR (a), post contrast coronal (b,c) and sagittal (d) MR images depict marrow signal alteration with heterogeneous post contrast enhancement in the frontal bone (arrow) and bilateral orbital roofs (dashed arrow) with associated enhancing subperiosteal (double arrow) and dural soft tissue (curved arrow) suggestive of osteomyelitis with pachymeningitis. Note made of left maxillary sinusitis (block arrow) with periantral inflammation (arrowhead).

diffusion with low mean apparent diffusion coefficient (ADC) while the centre of the abscess shows higher ADC values (Fig. 8). On MR Spectroscopy, multiple peaks are observed between 3.6 and 3.8 ppm corresponding to the metabolite trehalose present in the fungal wall [19,23]. Abscesses were most frequently encountered in the frontal (57.1%) and temporal lobes (28.6%) in our study group. This is in concurrence with Mishra et al who evaluated 90 patients with intracranial fungal infections in the pre-COVID era [24]. Similar distribution was described by Kaushik et al in their review article on CAM [19].

c) **Mucor emboli-** These are seen as multiple well defined round lesions with rim enhancement and central restriction of diffusion, at grey-white matter interface (Fig. 11). We encountered them most commonly in the middle cerebral artery territory (66.7%) similar to what has been previously reported in literature [25]. Micro-hemorrhages within the emboli may be seen as foci of blooming on SWI [19,25].

C) Meningeal involvement

Focal pachymeningitis is the most common form of meningeal involvement in CAM which presents as focal meningeal thickening and enhancement on imaging. Progression to arachnoiditis with resultant ventriculitis and hydrocephalus may occur [5]. Dural abscess formation may be seen (Fig. 12). Common sites for meningeal involvement include the paracavernous dura and dura along the frontal convexities (Fig. 6c, d and 12). Diffuse meningitis may very rarely be associated with CAM [19].

D) Bony involvement

Bone marrow involvement which is detected early on MR imaging, is seen as T1 hypointensity and T2/STIR hyperintensity with post contrast enhancement.

This may progress to rarefaction, frank erosions, fragmentation and sclerosis in chronic cases which is better depicted on CT. Apart from the skull base, cribriform plate of ethmoid is another common site of involvement (Figs. 12, 13). We also encountered one case of frank frontal bone osteomyelitis with subperiosteal abscess [12,19,26] (Fig. 14).

E) Perineural spread

Perineural spread, previously considered unusual is now an established route of disease spread to the brain. Nerve microenvironment and neurotropic factors secreted in a gradient along the nerve form the basis of perineural spread of fungus [27]. Histopathological evidence of perineural spread of ROCM has been reported in various studies [28,29]. However, only few case series have reported radiological evidence of the same, trigeminal nerve being the most commonly involved [29]. Signs of perineural spread of disease on MR imaging include irregular thickening and enhancement of the involved nerve. Obliteration of perineural fat pad and widening of neural foramen are ancillary findings [19,30] (Figs. 15-18). Muscles innervated by the cranial nerve may show denervation changes in the form of T2W hyperintensity and enhancement in the early stage and fatty change with volume loss in long-standing denervation [31] (Fig. 17).

In our experience, maxillary division was the most commonly involved nerve (37.9%) followed by the vidian nerve (13.8%). Main trigeminal nerve, its ophthalmic and mandibular divisions as well as facial nerve were the other involved nerves.

Nerve abscesses involving the mandibular and trigeminal nerves were observed in one patient each (Figs. 17, 18). Such florid

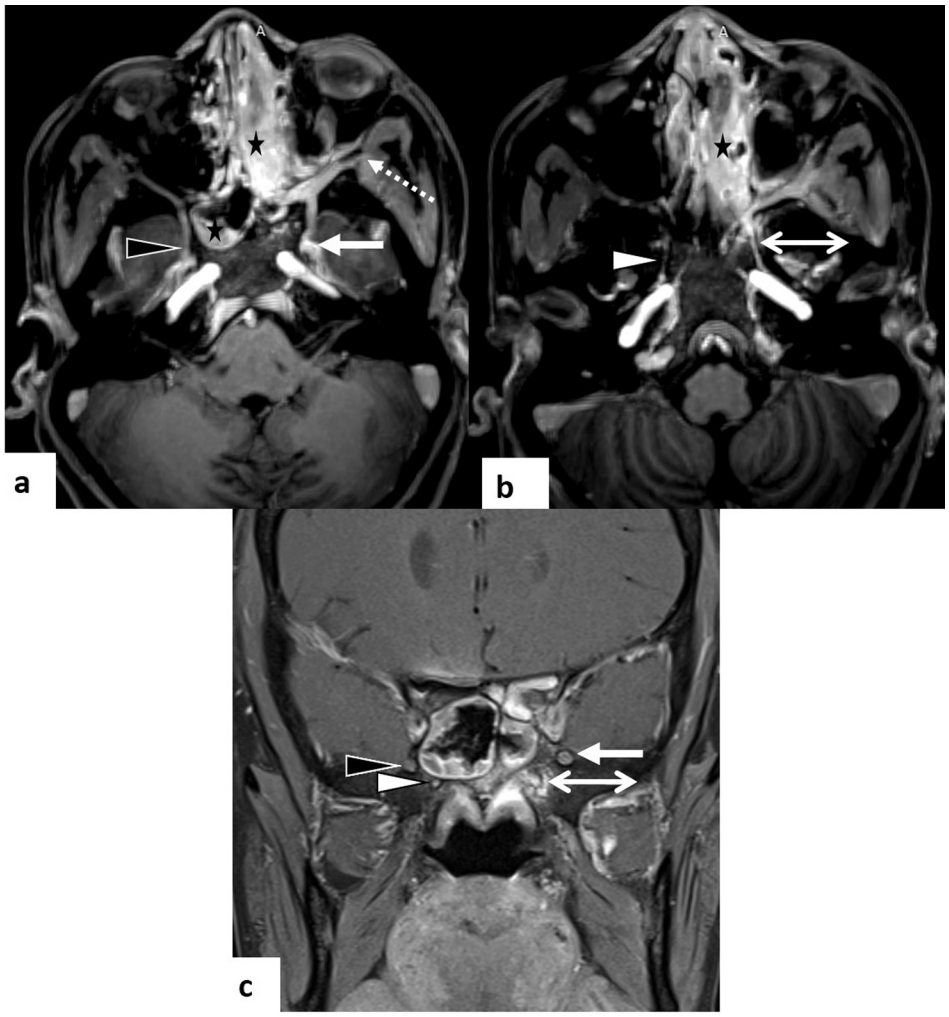

Fig. 15. Perineural spread along left maxillary and vidian nerves in CAM. Axial post-contrast MIP images (a,b) show thickening and enhancement of the left maxillary nerve in the region of the foramen rotundum and inferior orbital fissure (white solid and dashed arrow in a respectively) and vidian nerve (double white arrow in b). Coronal post contrast MPR image depicts the thickened nerves in the left foramen rotundum and vidian canal (arrow and double arrow respectively). Note made of normal right maxillary and vidian nerves (black and white arrowheads in a,b,c respectively). Ethmoid (L > R) and sphenoid sinusitis is noted (*).

involvement of cranial nerves in the form of full-blown abscesses is sparse in published literature.

4. Impact on patient prognosis

All 52 patients were prospectively followed up for 10–12 weeks after their scan. Although the morbidity was high, we observed a survival rate of 88.5% in our study. Out of the six deceased patients in our study, five patients had intracranial disease, all of whom had parenchymal and bone involvement. Survival rate in patients with intracranial disease was 82.8% (24/29 patients) in our study as compared to 20% and 47.8% reported in various studies in the pre-COVID era [8,23]. Overall no significant difference in patient outcome was seen in patients with and without intracranial involvement. This can be attributed to early initiation of antifungal therapy and prompt surgical management based on strong clinical and/or radiological suspicion even before histopathological confirmation was available to avoid delay in management. This is in agreement with Kumari et al who reported relatively good outcome in 20 patients of CAM in their study with a survival rate of 70% [32]. Brain parenchymal involvement was the only subset of intracranial disease that was significantly associated with higher mortality (p value 0.016).

5. Conclusion

CAM was the most dreaded aftermath of the second wave of the pandemic in India, challenging the already burdened health infrastructure of the country. It is crucial for radiologists to be familiar with the imaging manifestations of the disease. Prompt diagnosis and mapping of disease extent on imaging followed by aggressive treatment is imperative as histopathological results often take time. Intracranial disease is a potentially fatal complication of CAM and orbital apex is an important conduit of intracranial disease spread. In our experience, CAM including its intracranial complications had better prognosis as compared to ROCM in the pre-COVID era likely due to early initiation of treatment based on high index of suspicion in the pandemic and typical imaging findings. Every attempt must be made to check disease progression before brain parenchymal complications set in as these are harbingers of poor outcome.

Declaration of Competing Interest

The authors declare that they have no known competing financial interests or personal relationships that could have appeared to influence the work reported in this paper.

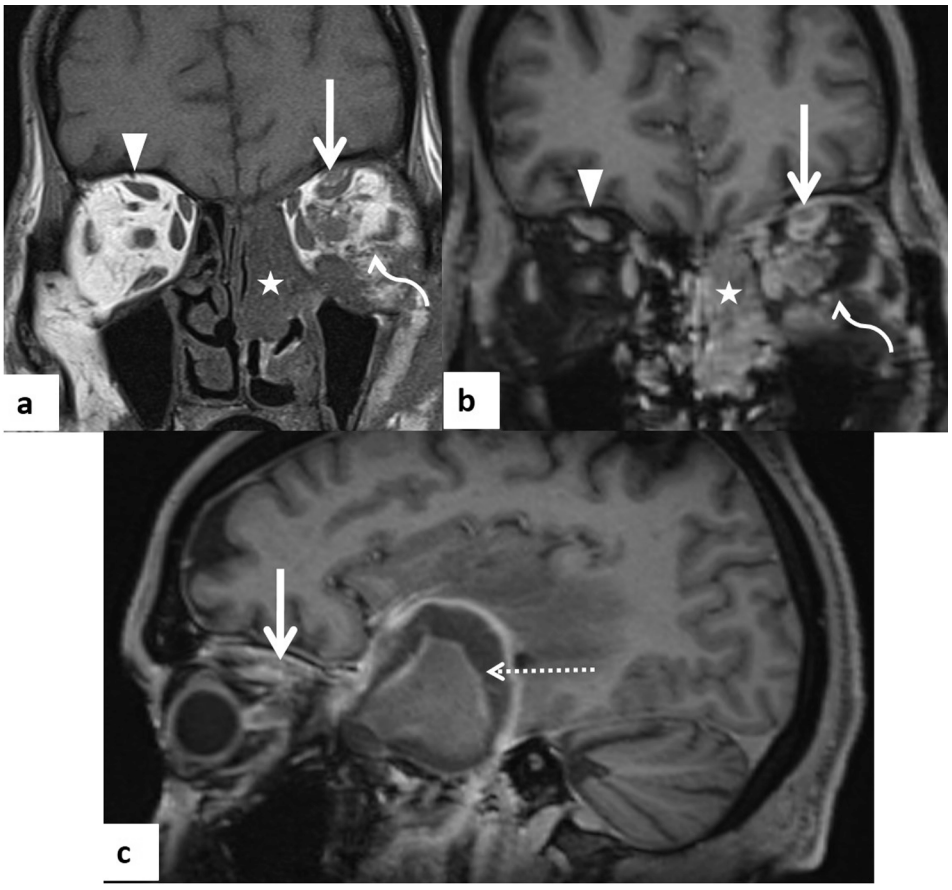

Fig. 16. Perineural spread along left ophthalmic nerve in CAM. Coronal T1W (a) and post contrast coronal (b) and sagittal (c) MR images reveal irregular thickening and enhancement of the left ophthalmic nerve (arrow) along the orbital roof above the superior rectus-levator palpebrae superioris complex indicating perineural spread of disease. Note the normal appearance of fat along the orbital roof on right (arrowhead in a,b). Left ethmoid sinusitis (* in a, b) along with orbital disease (curved arrow in a, b) and intraparenchymal brain abscess (dashed arrow in c) are noted.

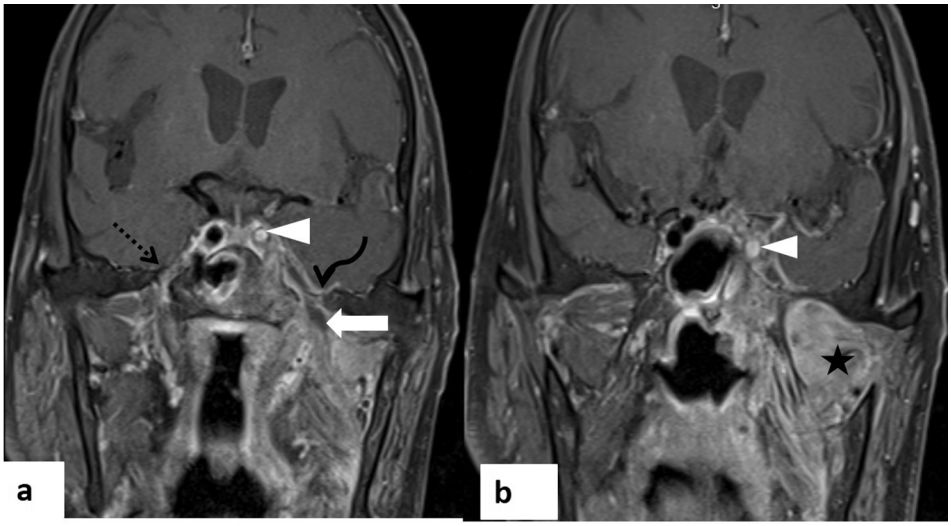

Fig. 17. Perineural spread with nerve abscess along left mandibular nerve in CAM. Coronal post contrast T1FS images (a,b) show rim enhancing abscess along the left mandibular nerve (arrow in a) with widening of the foramen ovale (curved arrow in a) and resultant acute denervation changes in muscles of mastication (* in b). Left cavernous sinus involvement with ICA thrombosis (arrowhead) is also seen. Note the normal right mandibular nerve (dashed arrow in a).

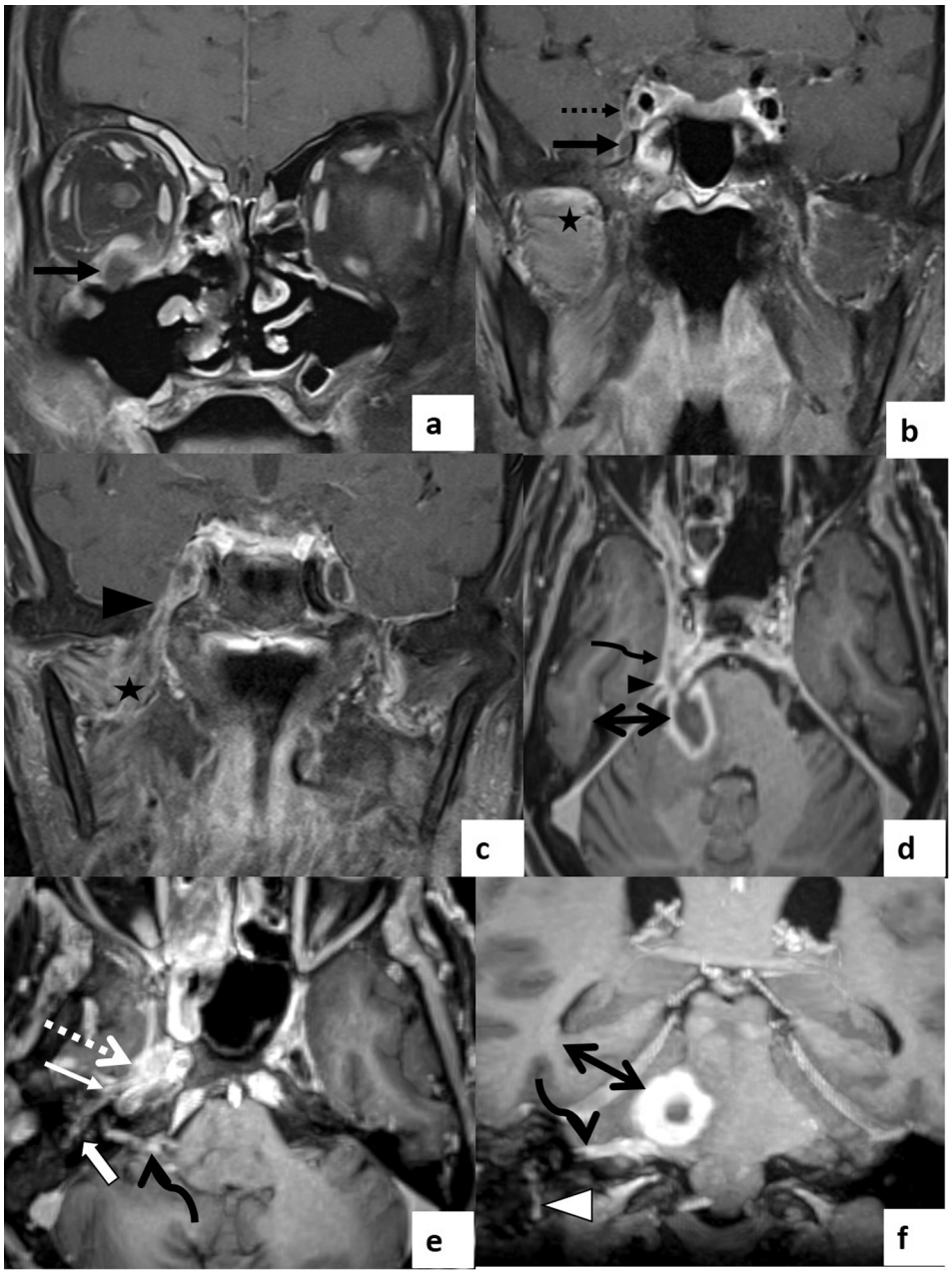

Fig. 18. Extensive perineural spread along the right trigeminal and facial nerves in CAM. Coronal post contrast T1FS MR images (a,b,c) from anterior to posterior show perineural spread along the right maxillary division at the level of the infraorbital foramen and cavernous sinus (arrow in a,b). Disease spread is also seen along the right ophthalmic division (dashed arrow in b), mandibular division (arrowhead in c) with denervation changes in the muscles of mastication (* in b,c). Axial post contrast image (d) demonstrates a rim enhancing abscess involving the Meckel's cave (curved arrow), cisternal segment (arrowhead) and pontine nucleus (double arrow) of the trigeminal nerve. Post contrast MIP images (e,f) show enhancement and thickening in the expected location of the greater superficial petrosal nerve (dashed arrow), extending into the genu (thin arrow), along the tympanic (thick arrow), mastoid (arrowhead in f) and cisternal (curved arrow) segments of the right facial nerve suggestive of perineural spread. Double arrow in f marks the nerve abscess involving the trigeminal nucleus.

References

[1] H. Elinav, O. Zimhony, M.J. Cohen, A.L. Marcovich, S. Benenson, Rhinocerebralmucormycosis in patients without predisposing medical conditions: a review of the literature, Clin. Microbiol. Infect. 15 (7) (2009) 693–697.

[2] A. Patel, H. Kaur, I. Xess, J.S. Michael, J. Savio, S. Rudramurthy, R. Singh, P. Shastri, P. Umabala, R. Sardana, A. Kindo, M.R. Capoor, S. Mohan, V. Muthu, R. Agarwal, A. Chakrabarti, A multicentre observational study on the epidemiology, risk factors, management and outcomes of mucormycosis in India, Clin. Microbiol. Infect. 26 (7) (2020).

[3] M. Sen, S.G. Honavar, R. Bansal, S. Sengupta, R. Rao, U. Kim, et al., Epidemiology, clinical profile, management, and outcome of COVID–19–associated rhino–orbital–cerebral mucormycosis in 2826 patients in India – Collaborative OPAI–IJO Study on Mucormycosis in COVID–19 (COSMIC), Report 1, Indian J. Ophthalmol. 69 (2021) 1670–1692.

[4] R. Meher, V. Wadhwa, V. Kumar, D. Shisha Phanbuh, R. Sharma, I. Singh, P. K. Rathore, R. Goel, R. Arora, S. Garg, S. Kumar, J. Kumar, M. Agarwal, M. Singh, N. Khurana, T. Sagar, V. Manchanda, S. Saxena, COVID associated mucormycosis: A preliminary study from a dedicated COVID Hospital in Delhi, Am. J. Otolaryngol. 43 (1) (2022) 103220.

[5] V. Pai, R. Sansi, R. Kharche, S.C. Bandili, B. Pai, Rhino-orbito-cerebral Mucormycosis: Pictorial Review, Insights into imaging. 12 (1) (2021) 1–7.

[6] A. Skied, I. Pavleas, M. Drogari-Apiranthitou, Epidemiology and diagnosis of mucormycosis: an update, J Fungi (Basel) 6 (2020) 265.

[7] Cornely OA, Alastruey-Izquierdo A, Arenz D, Chen SCA, Dannaoui E, Hochhegger B et al (2019) Global guideline for the diagnosis and management of mucormycosis: an initiative of the European Confederation of Medical Mycology in cooperation with the Mycoses Study Group Education and Research Consortium.Lancet Infect Dis 19:e405–e421.

[8] D.A. Herrera, A.B. Dublin, E.L. Ormsby, S. Aminpour, L.P. Howell, Imaging findings of rhinocerebral mucormycosis, Skull Base. 19 (2) (2009) 117–125.

[9] M. Aribandi, V.A. McCoy, C. Bazan, Imaging Features of Invasive and Noninvasive Fungal Sinusitis: A Review, RadioGraphics. 27 (5) (2007) 1283–1296.

[10] Safder S, Carpenter JS, Roberts TD, Bailey N (2009) The "Black Turbinate".

[11] sign: an early MR imaging finding of nasal mucormycosis. Am J Neuroradiol 31(4): 771–774.

[12] J. Therakathu, S. Prabhu, A. Irodi, S.V. Sudhakar, V.K. Yadav, V. Rupa, Imaging features of rhinocerebral mucormycosis: a study of 43 patients, Egypt. J. Radiol. Nucl. Med. 49 (2) (2018) 447–452.

[13] A. Chikley, R. Ben-Ami, D.P. Kontoyiannis, Mucormycosis of the central nervous system, J Fungi. 5 (3) (2019) 59.

[14] S. Manchanda, K. Semalti, A.S. Bhalla, A. Thakar, K. Sikka, H. Verma, Revisiting rhino-orbito-cerebral acute invasive fungal sinusitis in the era of COVID-19: pictorial review, Emerg. Radiol. 28 (6) (2021) 1063–1072.

[15] Khullar T, Kumar J, Sindhu D, Garg A, Meher R, Goel R. Coronavirus disease 2019 associated mucormycosis meandering its way into the orbit: a pictorial review. J Laryngol Otol 2021;1-5.
[16] A.L. Chaulk, T.H. Do, E.P. Supsupin, M.B. Bhattacharjee, K. Richani, O.-O. Adesina, A unique radiologic case of optic nerve infarction in a patient with mucormycosis, J. Neuroophthalmol. 41 (3) (2021).
[17] B. Galletti, F. Freni, A. Meduri, G.W. Oliverio, G.A. Signorino, P. Perroni, C. Galletti, P. Aragona, F. Galletti, Rhino-orbito-cerebral mucormycosis in diabetic disease mucormycosis in diabetic disease, J Craniofac Surg. 31 (4) (2020) e321–e324.
[18] K. Sharma, T. Tiwari, S. Goyal, R. Sharma, Rhino-orbito-cerebral mucormycosis causing cranial nerve abscess in post-COVID-19 status, BMJ Case Rep. 14 (9) (2021).
[19] T. Khullar, J. Kumar, D. Sindhu, A. Garg, R. Meher, CT Imaging Features in Acute Invasive Fungal Rhinosinusitis- Recalling the Oblivion in the COVID Era, Curr. Probl. Diagn. Radiol. (2022).
[20] K.S. Kaushik, R. Ananthasivan, U.V. Acharya, S. Rawat, U.D. Patil, B. Shankar, A. Jose, Spectrum of intracranial complications of rhino-orbito-cerebral mucormycosis—resurgence in the era of COVID-19 pandemic: a pictorial essay, Emerg. Radiol. 28 (6) (2021) 1097–1106.
[21] L. Mazzai, M. Anglani, C. Giraudo, M. Martucci, G. Cester, F. Causin, Imaging features of rhinocerebral mucormycosis: from onset to vascular complications, Acta Radiol. 63 (2) (2021) 232–244.
[22] P.A. Lone, N.A. Wani, M. Jehangir, Rhino-orbito-cerebral mucormycosis: magnetic resonance imaging, IndianJ Otol. 21 (3) (2015) 215.
[23] K.A. Fu, P.L. Nguyen, N. Sanossian, Basilar artery territory stroke secondary to invasive fungal sphenoid sinusitis: a case report and review of the literature, Case Rep Neurol. 7 (1) (2015) 51–58.
[24] G. Luthra, A. Parihar, K. Nath, S. Jaiswal, K.N. Prasad, N. Husain, M. Husain, S. Singh, S. Behari, R.K. Gupta, Comparative evaluation of fungal, tubercular, and pyogenic brain abscesses with conventional and diffusion MR imaging and proton MR spectroscopy, Am J Neuroradiol. 28 (7) (2007) 1332–1338.
[25] A. Mishra, A.R. Prabhuraj, D.P. Shukla, B.N. Nandeesh, N. Chandrashekar, A. Ramalingaiah, A. Arivazhagan, D.I. Bhat, S. Somanna, B.I. Devi, Intracranial fungal granuloma: a single-institute study of 90 cases over 18 years, Neurosurg. Focus 47 (2) (2019).
[26] M.A. Scully, G.A. Yeaney, M.L. Compton, M.J. Berg, SWAN MRI revealing multiple microhemorrhages secondary to septic emboli from mucormycosis, Neurology 79 (18) (2012) 1932–1933.
[27] L.L. Chan, S. Singh, D. Jones, E.M. Diaz Jr, L.E. Ginsberg, Imaging of mucormycosis skull base osteomyelitis, Am J Neuroradiol. 21 (5) (2000) 828–831.
[28] R.L. Bakst, N. Lee, S. He, N. Chernichenko, C.-H. Chen, G. Linkov, H.C. Le, J. Koutcher, E. Vakiani, R.J. Wong, K. Camphausen, Radiation impairs perineural invasion by modulating the nerve microenvironment, PLoS ONE 7 (6) (2012).
[29] F.M. McLean, L.E. Ginsberg, C.A. Stanton, Perineural spread of rhinocerebral mucormycosis, Am J Neuroradiol. 17 (1) (1996) 114–116.
[30] T. Sravani, S.G. Uppin, M.S. Uppin, C. Sundaram, Rhinocerebral mucormycosis: Pathology revisited with emphasis on perineural spread, Neurol India. 62 (4) (2014) 383.
[31] Zafer Koc, Filiz Koc, Deniz Yerdelen, Hakan Ozdogu, Rhino-orbital-cerebral mucormycosis with different cerebral involvements: infarct, hemorrhage, and ophthalmoplegia, Int. J. Neurosci. 117 (12) (2007) 1677–1690.
[32] N. Gupta, S. Dembla, Cranial nerve involvement in mucormycosis in post-COVID patients: a case series, Egypt. J. Radiol. Nucl. Med. 53 (2022) 28.
[33] A. Kumari, N.P. Rao, U. Patnaik, V. Malik, M.S. Tevatia, S. Thakur, J. Jaydevan, P. Saxena, Management outcomes of mucormycosis in COVID-19 patients: A preliminary report from a tertiary care hospital, Med J Armed Forces India. 77 (2021).